Flexible Models for Microclustering with Application to Entity Resolution

Giacomo Zanella[*]
Department of Decision Sciences
Bocconi University
giacomo.zanella@unibocconi.it

Brenda Betancourt[*]
Department of Statistical Science
Duke University
bb222@stat.duke.edu

Hanna Wallach
Microsoft Research
hanna@dirichlet.net

Jeffrey Miller
Department of Biostatistics
Harvard University
jwmiller@hsph.harvard.edu

Abbas Zaidi
Department of Statistical Science
Duke University
amz19@stat.duke.edu

Rebecca C. Steorts
Departments of Statistical Science and Computer Science
Duke University
beka@stat.duke.edu

Abstract

Most generative models for clustering implicitly assume that the number of data points in each cluster grows linearly with the total number of data points. Finite mixture models, Dirichlet process mixture models, and Pitman–Yor process mixture models make this assumption, as do all other infinitely exchangeable clustering models. However, for some applications, this assumption is inappropriate. For example, when performing entity resolution, the size of each cluster should be unrelated to the size of the data set, and each cluster should contain a negligible fraction of the total number of data points. These applications require models that yield clusters whose sizes grow sublinearly with the size of the data set. We address this requirement by defining the microclustering property and introducing a new class of models that can exhibit this property. We compare models within this class to two commonly used clustering models using four entity-resolution data sets.

1 Introduction

Many clustering applications require models that assume cluster sizes grow linearly with the size of the data set. These applications include topic modeling, inferring population structure, and discriminating among cancer subtypes. Infinitely exchangeable clustering models, including finite mixture models, Dirichlet process mixture models, and Pitman–Yor process mixture models, all make this linear-growth assumption, and have seen numerous successes when used in these contexts. For other clustering applications, such as entity resolution, this assumption is inappropriate. Entity resolution (including record linkage and de-duplication) involves identifying duplicate[2] records in noisy databases [1, 2], traditionally by directly linking records to one another. Unfortunately, this traditional approach is computationally infeasible for large data sets—a serious limitation in "the age of big data" [1, 3]. As a

---

[*]Giacomo Zanella and Brenda Betancourt are joint first authors.

[2]In the entity resolution literature, the term "duplicate records" does not mean that the records are identical, but rather that the records are corrupted, degraded, or otherwise noisy representations of the same entity.

result, researchers increasingly treat entity resolution as a clustering problem, where each entity is implicitly associated with one or more records and the inference goal is to recover the latent entities (clusters) that correspond to the observed records (data points) [4, 5, 6]. In contrast to other clustering applications, the number of data points in each cluster should remain small, even for large data sets. Applications like this require models that yield clusters whose sizes grow sublinearly with the total number of data points [7]. To address this requirement, we define the microclustering property in section 2 and, in section 3, introduce a new class of models that can exhibit this property. In section 4, we compare two models within this class to two commonly used infinitely exchangeable clustering models.

2 The Microclustering Property

To cluster N data points $x_1, \ldots, x_N$ using a partition-based Bayesian clustering model, one first places a prior over partitions of $[N] = \{1, \ldots, N\}$. Then, given a partition C_N of $[N]$, one models the data points in each part $c \in C_N$ as jointly distributed according to some chosen distribution. Finally, one computes the posterior distribution over partitions and, e.g., uses it to identify probable partitions of $[N]$. Mixture models are a well-known type of partition-based Bayesian clustering model, in which C_N is implicitly represented by a set of cluster assignments $z_1, \ldots, z_N$. These cluster assignments can be regarded as the first N elements of an infinite sequence $z_1, z_2, \ldots$, drawn a priori from

$$\boldsymbol{\pi} \sim H \quad \text{and} \quad z_1, z_2, \ldots \mid \boldsymbol{\pi} \stackrel{\text{iid}}{\sim} \boldsymbol{\pi}, \tag{1}$$

where H is a prior over $\boldsymbol{\pi}$ and $\boldsymbol{\pi}$ is a vector of mixture weights with $\sum_l \pi_l = 1$ and $\pi_l \geq 0$ for all l. Commonly used mixture models include (a) finite mixtures where the dimensionality of $\boldsymbol{\pi}$ is fixed and H is usually a Dirichlet distribution; (b) finite mixtures where the dimensionality of $\boldsymbol{\pi}$ is a random variable [8, 9]; (c) Dirichlet process (DP) mixtures where the dimensionality of $\boldsymbol{\pi}$ is infinite [10]; and (d) Pitman–Yor process (PYP) mixtures, which generalize DP mixtures [11].

Equation 1 implicitly defines a prior over partitions of $\mathbb{N} = \{1, 2, \ldots\}$. Any random partition $C_\mathbb{N}$ of $\mathbb{N}$ induces a sequence of random partitions $(C_N : N = 1, 2, \ldots)$, where C_N is a partition of $[N]$. Via the strong law of large numbers, the cluster sizes in any such sequence obtained via equation 1 grow linearly with N because, with probability one, for all l, $\frac{1}{N} \sum_{n=1}^N I(z_n = l) \to \pi_l$ as $N \to \infty$, where $I(\cdot)$ denotes the indicator function. Unfortunately, this linear growth assumption is not appropriate for entity resolution and other applications that require clusters whose sizes grow sublinearly with N.

To address this requirement, we therefore define the microclustering property: A sequence of random partitions $(C_N : N = 1, 2, \ldots)$ exhibits the microclustering property if M_N is $o_p(N)$, where M_N is the size of the largest cluster in C_N, or, equivalently, if $M_N / N \to 0$ in probability as $N \to \infty$.

A clustering model exhibits the microclustering property if the sequence of random partitions implied by that model satisfies the above definition. No mixture model can exhibit the microclustering property (unless its parameters are allowed to vary with N). In fact, Kingman's paintbox theorem [12, 13] implies that any exchangeable partition of $\mathbb{N}$, such as a partition obtained using equation 1, is either equal to the trivial partition in which each part contains one element or satisfies $\liminf_{N \to \infty} M_N / N > 0$ with positive probability. By Kolmogorov's extension theorem, a sequence of random partitions $(C_N : N = 1, 2, \ldots)$ corresponds to an exchangeable random partition of $\mathbb{N}$ whenever (a) each C_N is finitely exchangeable (i.e., its probability is invariant under permutations of $\{1, \ldots, N\}$) and (b) the sequence is projective (also known as consistent in distribution)—i.e., if $N' < N$, the distribution over $C_{N'}$ coincides with the marginal distribution over partitions of $[N']$ induced by the distribution over C_N. Therefore, to obtain a nontrivial model that exhibits the microclustering property, we must sacrifice either (a) or (b). Previous work [14] sacrificed (a); in this paper, we instead sacrifice (b).

Sacrificing finite exchangeability and sacrificing projectivity have very different consequences. If a partition-based Bayesian clustering model is not finitely exchangeable, then inference will depend on the order of the data points. For most applications, this consequence is undesirable—there is no reason to believe that the order of the data points is meaningful. In contrast, if a model lacks projectivity, then the implied joint distribution over a subset of the data points in a data set will not be the same as the joint distribution obtained by modeling the subset directly. In the context of entity resolution, sacrificing projectivity is a more natural and less restrictive choice than sacrificing finite exchangeability.

3 Kolchin Partition Models for Microclustering

We introduce a new class of Bayesian models for microclustering by placing a prior on the number of clusters K and, given K, modeling the cluster sizes $N_1, \ldots, N_K$ directly. We start by defining

$$K \sim \boldsymbol{\kappa} \quad \text{and} \quad N_1, \ldots, N_K \,|\, K \overset{\text{iid}}{\sim} \boldsymbol{\mu}, \tag{2}$$

where $\boldsymbol{\kappa} = (\kappa_1, \kappa_2, \ldots)$ and $\boldsymbol{\mu} = (\mu_1, \mu_2, \ldots)$ are probability distributions over $\mathbb{N} = \{1, 2, \ldots\}$. We then define $N = \sum_{k=1}^{K} N_k$ and, given $N_1, \ldots, N_K$, generate a set of cluster assignments $z_1, \ldots, z_N$ by drawing a vector uniformly at random from the set of permutations of $(\underbrace{1, \ldots, 1}_{N_1 \text{ times}}, \underbrace{2, \ldots, 2}_{N_2 \text{ times}}, \ldots\ldots, \underbrace{K, \ldots, K}_{N_K \text{ times}})$. The cluster assignments $z_1, \ldots, z_N$ induce a random partition C_N of $[N]$, where N is itself a random variable—i.e., C_N is a random partition of a random number of elements. We refer to the resulting class of marginal distributions over C_N as Kolchin partition (KP) models [15, 16] because the form of equation 2 is closely related to Kolchin's representation theorem for Gibbs-type partitions (see, e.g., 16, theorem 1.2). For appropriate choices of $\boldsymbol{\kappa}$ and $\boldsymbol{\mu}$, KP models can exhibit the microclustering property (see appendix B for an example).

If $\mathscr{C}_N$ denotes the set of all possible partitions of $[N]$, then $\bigcup_{N=1}^{\infty} \mathscr{C}_N$ is the set of all possible partitions of $[N]$ for all $N \in \mathbb{N}$. The probability of any given partition $C_N \in \bigcup_{N=1}^{\infty} \mathscr{C}_N$ is

$$P(C_N) = \frac{|C_N|! \, \kappa_{|C_N|}}{N!} \left(\prod_{c \in C_N} |c|! \, \mu_{|c|} \right), \tag{3}$$

where $|\cdot|$ denotes the cardinality of a set, $|C_N|$ is the number of clusters in C_N, and $|c|$ is the number of elements in cluster c. In practice, however, N is usually observed. Conditioned on N, a KP model implies that $P(C_N \,|\, N) \propto |C_N|! \, \kappa_{|C_N|} \left(\prod_{c \in C_N} |c|! \, \mu_{|c|} \right)$. Equation 3 leads to a "reseating algorithm"—much like the Chinese restaurant process (CRP)—derived by sampling from $P(C_N \,|\, N, C_N \backslash n)$, where $C_N \backslash n$ is the partition obtained by removing element n from C_N:

- for $n = 1, \ldots, N$, reassign element n to
    - an existing cluster $c \in C_N \backslash n$ with probability $\propto (|c| + 1) \frac{\mu_{(|c|+1)}}{\mu_{|c|}}$
    - or a new cluster with probability $\propto (|C_N \backslash n| + 1) \frac{\kappa_{(|C_N \backslash n|+1)}}{\kappa_{|C_N \backslash n|}} \mu_1$.

We can use this reseating algorithm to draw samples from $P(C_N \,|\, N)$; however, unlike the CRP, it does not produce an exact sample if it is used to incrementally construct a partition from the empty set. In practice, this limitation does not lead to any negative consequences because standard posterior inference sampling methods do not rely on this property. When a KP model is used as the prior in a partition-based clustering model—e.g., as an alternative to equation 1—the resulting Gibbs sampling algorithm for C_N is similar to this reseating algorithm, but accompanied by likelihood terms. Unfortunately, this algorithm is slow for large data sets. In appendix C, we therefore propose a faster Gibbs sampling algorithm—the chaperones algorithm—that is particularly well suited to microclustering.

In sections 3.1 and 3.2, we introduce two related KP models for microclustering, and in section 3.4 we explain how KP models can be applied in the context of entity resolution with categorical data.

3.1 The NBNB Model

We start with equation 3 and define

$$\boldsymbol{\kappa} = \text{NegBin}\,(a, q) \quad \text{and} \quad \boldsymbol{\mu} = \text{NegBin}\,(r, p), \tag{4}$$

where $\text{NegBin}(a, q)$ and $\text{NegBin}(r, p)$ are negative binomial distributions truncated to $\mathbb{N} = \{1, 2, \ldots\}$. We assume that $a > 0$ and $q \in (0, 1)$ are fixed hyperparameters, while r and p are distributed as $r \sim \text{Gam}(\eta_r, s_r)$ and $p \sim \text{Beta}(u_p, v_p)$ for fixed η_r, s_r, u_p and v_p.[3] We refer to the resulting marginal distribution over C_N as the negative binomial–negative binomial (NBNB) model.

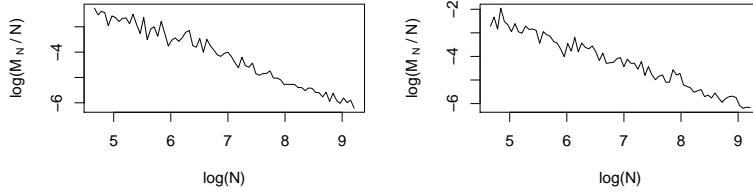[3]We use the shape-and-rate parameterization of the gamma distribution.

Figure 1: The NBNB (left) and NBD (right) models appear to exhibit the microclustering property.

By substituting equation 4 into equation 3, we obtain the probability of C_N conditioned N:

$$P(C_N \mid N, a, q, r, p) \propto \Gamma\left(|C_N| + a\right) \beta^{|C_N|} \prod_{c \in C_N} \frac{\Gamma\left(|c| + r\right)}{\Gamma\left(r\right)}, \tag{5}$$

where $\beta = \frac{q\,(1-p)^r}{1-(1-p)^r}$. We provide the complete derivation of equation 5, along with the conditional posterior distributions over r and p, in appendix A.2. Posterior inference for the NBNB model involves alternating between (a) sampling C_N from $P(C_N \mid N, a, q, r, p)$ using the chaperones algorithm and (b) sampling r and p from their respective conditional posteriors using, e.g., slice sampling [17].

3.2 The NBD Model

Although $\boldsymbol{\kappa} = \text{NegBin}\,(a, q)$ will yield plausible values of K, $\boldsymbol{\mu} = \text{NegBin}\,(r, p)$ may not be sufficiently flexible to capture realistic properties of $N_1, \ldots, N_K$, especially when K is large. For example, in a record-linkage application involving two otherwise noise-free databases containing thousands of records, K will be large and each N_k will be at most two. A negative binomial distribution cannot capture this property. We therefore define a second KP model—the negative binomial–Dirichlet (NBD) model—by taking a nonparametric approach to modeling $N_1, \ldots, N_K$ and drawing $\boldsymbol{\mu}$ from an infinite-dimensional Dirichlet distribution over the positive integers:

$$\boldsymbol{\kappa} = \text{NegBin}\,(a, q) \quad \text{and} \quad \boldsymbol{\mu} \mid \alpha, \boldsymbol{\mu}^{(0)} \sim \text{Dir}\left(\alpha, \boldsymbol{\mu}^{(0)}\right), \tag{6}$$

where $\alpha > 0$ is a fixed concentration parameter and $\boldsymbol{\mu}^{(0)} = (\mu_1^{(0)}, \mu_2^{(0)}, \cdots)$ is a fixed base measure with $\sum_{m=1}^{\infty} \mu_m^{(0)} = 1$ and $\mu_m^{(0)} \geq 0$ for all m. The probability of C_N conditioned on N and $\boldsymbol{\mu}$ is

$$P(C_N \mid N, a, q, \boldsymbol{\mu}) \propto \Gamma\left(|C_N| + a\right) q^{|C_N|} \prod_{c \in C_N} |c|!\, \mu_{|c|}. \tag{7}$$

Posterior inference for the NBD model involves alternating between (a) sampling C_N from $P(C_N \mid N, a, q, \boldsymbol{\mu})$ using the chaperones algorithm and (b) sampling $\boldsymbol{\mu}$ from its conditional posterior:

$$\boldsymbol{\mu} \mid C_N, \alpha, \boldsymbol{\mu}^{(0)} \sim \text{Dir}\left(\alpha\,\mu_1^{(0)} + L_1, \alpha\,\mu_2^{(0)} + L_2, \ldots\right), \tag{8}$$

where L_m is the number of clusters of size m in C_N. Although $\boldsymbol{\mu}$ is an infinite-dimensional vector, only the first N elements affect $P(C_N \mid a, q, \boldsymbol{\mu})$. Therefore, it is sufficient to sample the $(N + 1)$-dimensional vector $(\mu_1, \ldots, \mu_N, 1 - \sum_{m=1}^{N} \mu_m)$ from equation 8, modified accordingly, and retain only $\mu_1, \ldots, \mu_N$. We provide complete derivations of equations 7 and 8 in appendix A.3.

3.3 The Microclustering Property for the NBNB and NBD Models

Figure 1 contains empirical evidence suggesting that the NBNB and NBD models both exhibit the microclustering property. For each model, we generated samples of M_N / N for $N = 100, \ldots, 10^4$. For the NBNB model, we set $a = 1$, $q = 0.5$, $r = 1$, and $p = 0.5$ and generated the samples using rejection sampling. For the NBD model, we set $a = 1$, $q = 0.5$, and $\alpha = 1$ and set $\boldsymbol{\mu}^{(0)}$ to be a geometric distribution over $\mathbb{N} = \{1, 2, \ldots\}$ with a parameter of 0.5. We generated the samples using MCMC methods. For both models, M_N / N appears to converge to zero in probability as $N \to \infty$, as desired.

In appendix B, we also prove that a variant of the NBNB model exhibits the microclustering property.

4

3.4 Application to Entity Resolution

KP models can be used to perform entity resolution. In this context, the data points $x_1, \ldots, x_N$ are observed records and the K clusters are latent entities. If each record consists of F categorical fields, then

$$C_N \sim \text{KP model} \tag{9}$$

$$\boldsymbol{\theta}_{fk} \,|\, \delta_f, \boldsymbol{\gamma}_f \sim \text{Dir}\left(\delta_f, \boldsymbol{\gamma}_f\right) \tag{10}$$

$$z_n \sim \zeta(C_N, n) \tag{11}$$

$$x_{fn} \,|\, z_n, \boldsymbol{\theta}_{f1}, \ldots, \boldsymbol{\theta}_{fK} \sim \text{Cat}\left(\boldsymbol{\theta}_{fz_n}\right) \tag{12}$$

for $f = 1, \ldots, F$, $k = 1, \ldots, K$, and $n = 1, \ldots, N$, where $\zeta(C_N, n)$ maps the nth record to a latent cluster assignment z_n according to C_N. We assume that $\delta_f > 0$ is distributed as $\delta_f \sim \text{Gam}\left(1, 1\right)$, while $\boldsymbol{\gamma}_f$ is fixed. Via Dirichlet–multinomial conjugacy, we can marginalize over $\boldsymbol{\theta}_{11}, \ldots, \boldsymbol{\theta}_{FK}$ to obtain a closed-form expression for $P(x_1, \ldots, x_N \,|\, z_1, \ldots, z_N, \delta_f, \boldsymbol{\gamma}_f)$. Posterior inference involves alternating between (a) sampling C_N from $P(C_N \,|\, x_1, \ldots, x_N, \delta_f)$ using the chaperones algorithm accompanied by appropriate likelihood terms, (b) sampling the parameters of the KP model from their conditional posteriors, and (c) sampling δ_f from its conditional posterior using slice sampling.

4 Experiments

In this section, we compare two entity resolution models based on the NBNB model and the NBD model to two similar models based on the DP mixture model [10] and the PYP mixture model [11]. All four models use the likelihood in equations 10 and 12. For the NBNB model and the NBD model, we set a and q to reflect a weakly informative prior belief that $\mathbb{E}[K] = \sqrt{\text{Var}[K]} = \frac{N}{2}$. For the NBNB model, we set $\eta_r = s_r = 1$ and $u_p = v_p = 2$.[4] For the NBD model, we set $\alpha = 1$ and set $\boldsymbol{\mu}^{(0)}$ to be a geometric distribution over $\mathbb{N} = \{1, 2, \ldots\}$ with a parameter of 0.5. This base measure reflects a prior belief that $\mathbb{E}[N_k] = 2$. Finally, to ensure a fair comparison between the two different classes of model, we set the DP and PYP concentration parameters to reflect a prior belief that $\mathbb{E}[K] = \frac{N}{2}$.

We assess how well each model "fits" four data sets typical of those arising in real-world entity resolution applications. For each data set, we consider four statistics: (a) the number of singleton clusters, (b) the maximum cluster size, (c) the mean cluster size, and (d) the 90th percentile of cluster sizes. We compare each statistic's true value to its posterior distribution according to each of the models. For each model and data set combination, we also consider five entity-resolution summary statistics: (a) the posterior expected number of clusters, (b) the posterior standard error, (c) the false negative rate, (d) the false discovery rate, and (e) the posterior expected value of $\delta_f = \delta$ for $f = 1, \ldots, F$. The false negative and false discovery rates are both invariant under permutations of $1, \ldots, K$ [5, 18].

4.1 Data Sets

We constructed four realistic data sets, each consisting of N records associated with K entities.

Italy: We derived this data set from the Survey on Household Income and Wealth, conducted by the Bank of Italy every two years. There are nine categorical fields, including year of birth, employment status, and highest level of education attained. Ground truth is available via unique identifiers based upon social security numbers; roughly 74% of the clusters are singletons. We used the 2008 and 2010 databases from the Fruili region to create a record-linkage data set consisting of $N = 789$ records; each N_k is at most two. We discarded the records themselves, but preserved the number of fields, the empirical distribution of categories for each field, the number of clusters, and the cluster sizes. We then generated synthetic records using equations 10 and 12. We created three variants of this data set, corresponding to $\delta = 0.02, 0.05, 0.1$. For all three, we used the empirical distribution of categories for field f as $\boldsymbol{\gamma}_f$. By generating synthetic records in this fashion, we preserve the pertinent characteristics of the original data, while making it easy to isolate the impacts of the different priors over partitions.

NLTCS5000: We derived this data set from the National Long Term Care Survey (NLTCS)[5]—a longitudinal survey of older Americans, conducted roughly every six years. We used four of the

---

[4]We used $p \sim \text{Beta}\left(2, 2\right)$ because a uniform prior implies an unrealistic prior belief that $\mathbb{E}[N_k] = \infty$.
[5]http://www.nltcs.aas.duke.edu/

available fields: date of birth, sex, state of residence, and regional office. We split date of birth into three separate fields: day, month, and year. Ground truth is available via social security numbers; roughly 68% of the clusters are singletons. We used the 1982, 1989, and 1994 databases and down-sampled the records, preserving the proportion of clusters of each size and the maximum cluster size, to create a record-linkage data set of $N = 5,000$ records; each N_k is at most three. We then generated synthetic records using the same approach that we used to create the Italy data set.

Syria2000 and SyriaSizes: We constructed these data sets from data collected by four human-rights groups between 2011 and 2014 on people killed in the Syrian conflict [19, 20]. Hand-matched ground truth is available from the Human Rights Data Analysis Group. Because the records were hand matched, the data are noisy and potentially biased. Performing entity resolution is non-trivial because there are only three categorical fields: gender, governorate, and date of death. We split date of death, which is present for most records, into three separate fields: day, month, and year. However, because the records only span four years, the year field conveys little information. In addition, most records are male, and there are only fourteen governorates. We created the Syria2000 data set by down-sampling the records, preserving the proportion of clusters of each size, to create a data set of $N = 2,000$ records; the maximum cluster size is five. We created the SyriaSizes data set by down-sampling the records, preserving some of the larger clusters (which necessarily contain within-database duplications), to create a data set of $N = 6,700$ records; the maximum cluster size is ten. We provide the empirical distribution over cluster sizes for each data set in appendix D. We generated synthetic records for both data sets using the same approach that we used to create the Italy data set.
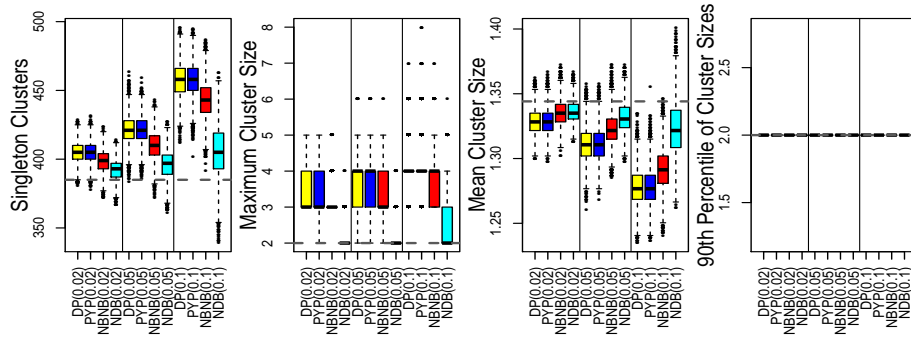
4.2 Results

We report the results of our experiments in table 1 and figure 2. The NBNB and NBD models outperformed the DP and PYP models for almost all variants of the Italy and NLTCS5000 data sets. In general, the NBD model performed the best of the four, and the differences between the models' performance grew as the value of δ increased. For the Syria2000 and SyriaSizes data sets, we see no consistent pattern to the models' abilities to recover the true values of the data-set statistics. Moreover, all four models had poor false negative rates, and false discovery rates—most likely because these data sets are extremely noisy and contain very few fields. We suspect that no entity resolution model would perform well for these data sets. For three of the four data sets, the exception being the Syria2000 data set, the DP model and the PYP model both greatly overestimated the number of clusters for larger values of δ. Taken together, these results suggest that the flexibility of the NBNB and NBD models make them more appropriate choices for most entity resolution applications.
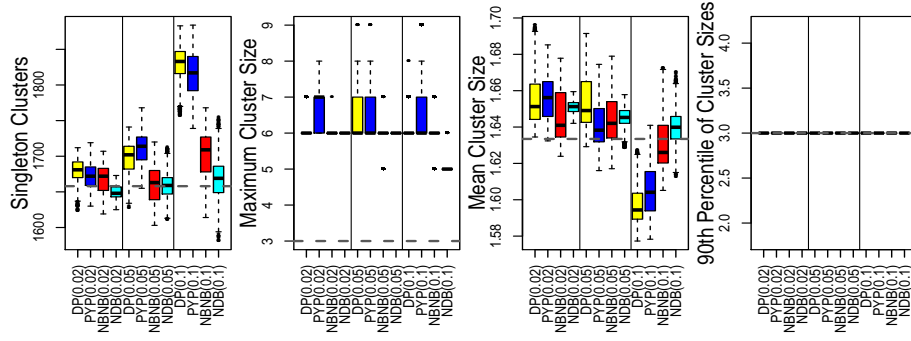
5 Summary

Infinitely exchangeable clustering models assume that cluster sizes grow linearly with the size of the data set. Although this assumption is reasonable for some applications, it is inappropriate for others. For example, when entity resolution is treated as a clustering problem, the number of data points in each cluster should remain small, even for large data sets. Applications like this require models that yield clusters whose sizes grow sublinearly with the size of the data set. We introduced the microclustering property as one way to characterize models that address this requirement. We then introduced a highly flexible class of models—KP models—that can exhibit this property. We presented two models within this class—the NBNB model and the NBD model—and showed that they are better suited to entity resolution applications than two infinitely exchangeable clustering models. We therefore recommend KP models for applications where the size of each cluster should be unrelated to the size of the data set, and each cluster should contain a negligible fraction of the total number of data points.

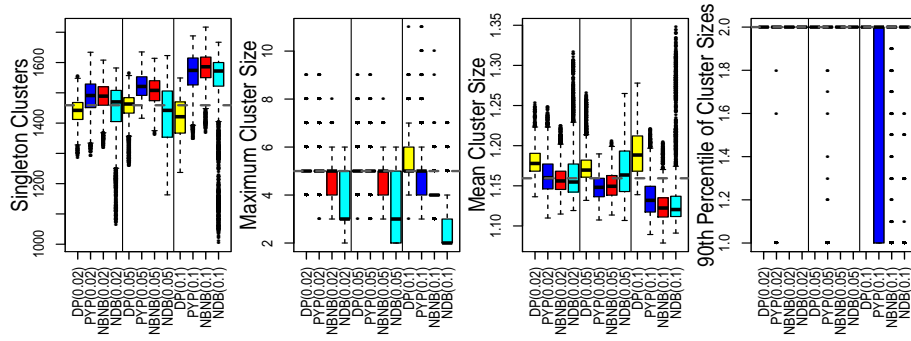(a) Italy: NBD model > NBNB model > PYP mixture model > DP mixture model.

(b) NLTCS5000: NBD model > NBNB model > PYP mixture model > DP mixture model.

(c) Syria2000: the models perform similarly because there are so few fields.
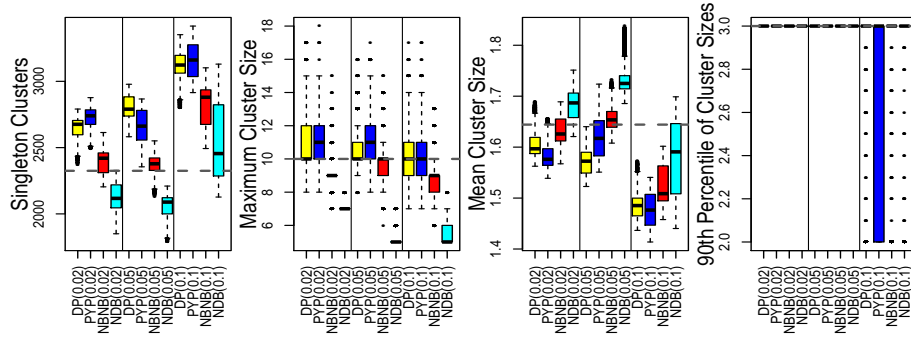
(d) SyriaSizes: the models perform similarly because there are so few fields.

Figure 2: Box plots depicting the true value (dashed line) of each data-set statistic for each variant of each data set, as well as its posterior distribution according to each of the four entity resolution models.

Table 1: Entity-resolution summary statistics—the posterior expected number of clusters, the posterior standard error, the false negative rate (lower is better), the false discovery rate (lower is better), and the posterior expected value of δ—for each variant of each data set and each of the four models.

Data Set	True K	Variant	Model	$\mathbb{E}[K]$	Std. Err.	FNR	FDR	$\mathbb{E}[\delta]$
Italy	587	$\delta = 0.02$	DP	594.00	4.51	0.07	0.03	0.02
			PYP	593.90	4.52	0.07	0.03	0.02
			NBNB	591.00	4.43	0.04	0.03	0.02
			NBD	590.50	3.64	0.03	0.00	0.02
		$\delta = 0.05$	DP	601.60	5.89	0.13	0.03	0.03
			PYP	601.50	5.90	0.13	0.03	0.04
			NBNB	596.40	5.79	0.11	0.04	0.04
			NBD	592.60	5.20	0.09	0.04	0.04
		$\delta = 0.1$	DP	617.40	7.23	0.27	0.06	0.07
			PYP	617.40	7.22	0.27	0.05	0.07
			NBNB	610.90	7.81	0.24	0.06	0.08
			NBD	596.60	9.37	0.18	0.05	0.10
NLTCS5000	3,061	$\delta = 0.02$	DP	3021.70	24.96	0.02	0.11	0.03
			PYP	3018.70	25.69	0.03	0.11	0.03
			NBNB	3037.80	25.18	0.02	0.07	0.02
			NBD	3028.20	5.65	0.01	0.09	0.03
		$\delta = 0.05$	DP	3024.00	26.15	0.05	0.13	0.06
			PYP	3045.80	23.66	0.05	0.10	0.05
			NBNB	3040.90	24.86	0.04	0.06	0.05
			NBD	3039.30	10.17	0.03	0.07	0.06
		$\delta = 0.1$	DP	3130.50	21.44	0.12	0.09	0.10
			PYP	3115.10	25.73	0.13	0.10	0.10
			NBNB	3067.30	25.31	0.11	0.08	0.11
			NBD	3049.10	16.48	0.09	0.08	0.12
Syria2000	1,725	$\delta = 0.02$	DP	1695.20	25.40	0.70	0.27	0.07
			PYP	1719.70	36.10	0.71	0.26	0.04
			NBNB	1726.80	27.96	0.70	0.28	0.05
			NBD	1715.20	51.56	0.67	0.28	0.02
		$\delta = 0.05$	DP	1701.80	31.15	0.77	0.31	0.07
			PYP	1742.90	24.33	0.75	0.32	0.04
			NBNB	1738.30	25.48	0.74	0.31	0.04
			NBD	1711.40	47.10	0.69	0.32	0.03
		$\delta = 0.1$	DP	1678.10	40.56	0.81	0.19	0.18
			PYP	1761.20	39.38	0.81	0.22	0.08
			NBNB	1779.40	29.84	0.77	0.26	0.04
			NBD	1757.30	73.60	0.74	0.25	0.03
SyriaSizes	4,075	$\delta = 0.02$	DP	4175.70	66.04	0.65	0.17	0.01
			PYP	4234.30	68.55	0.64	0.19	0.01
			NBNB	4108.70	70.56	0.65	0.19	0.01
			NBD	3979.50	70.85	0.68	0.20	0.03
		$\delta = 0.05$	DP	4260.00	77.18	0.71	0.21	0.02
			PYP	4139.10	104.22	0.75	0.18	0.04
			NBNB	4047.10	55.18	0.73	0.20	0.04
			NBD	3863.90	68.05	0.75	0.22	0.07
		$\delta = 0.1$	DP	4507.40	82.27	0.80	0.19	0.03
			PYP	4540.30	100.53	0.80	0.20	0.03
			NBNB	4400.60	111.91	0.80	0.23	0.03
			NBD	4251.90	203.23	0.82	0.25	0.04

References

[1] P. Christen. *Data Matching: Concepts and Techniques for Record Linkage, Entity Resolution, and Duplicate Detection*. Springer, 2012.

[2] P. Christen. A survey of indexing techniques for scalable record linkage and deduplication. *IEEE Transactions on Knowledge and Data Engineering*, 24(9), 2012.

[3] W. E. Winkler. Overview of record linkage and current research directions. Technical report, U.S. Bureau of the Census Statistical Research Division, 2006.

[4] R. C. Steorts, R. Hall, and S. E. Fienberg. A Bayesian approach to graphical record linkage and de-duplication. *Journal of the American Statistical Society*, In press.

[5] R. C. Steorts. Entity resolution with empirically motivated priors. *Bayesian Analysis*, 10(4): 849–875, 2015.

[6] R. C. Steorts, R. Hall, and S. E. Fienberg. SMERED: A Bayesian approach to graphical record linkage and de-duplication. *Journal of Machine Learning Research*, 33:922–930, 2014.

[7] T. Broderick and R. C. Steorts. Variational bayes for merging noisy databases. In *NIPS 2014 Workshop on Advances in Variational Inference*, 2014. arXiv:1410.4792.

[8] S. Richardson and P. J. Green. On Bayesian analysis of mixtures with an unknown number of components. *Journal of the Royal Statistical Society Series B*, pages 731–792, 1997.

[9] J. W. Miller and M. T. Harrison. Mixture models with a prior on the number of components. arXiv:1502.06241, 2015.

[10] J. Sethuraman. A constructive definition of Dirichlet priors. *Statistica Sinica*, 4:639–650, 1994.

[11] H. Ishwaran and L. F. James. Generalized weighted Chinese restaurant processes for species sampling mixture models. *Statistica Sinica*, 13(4):1211–1236, 2003.

[12] J. F. .C Kingman. The representation of partition structures. *Journal of the London Mathematical Society*, 2(2):374–380, 1978.

[13] D. Aldous. Exchangeability and related topics. *École d'Été de Probabilités de Saint-Flour XIII—1983*, pages 1–198, 1985.

[14] H. M. Wallach, S. Jensen, L. Dicker, and K. A. Heller. An alternative prior process for nonparametric Bayesian clustering. In *Proceedings of the 13th International Conference on Artificial Intelligence and Statistics*, 2010.

[15] V. F. Kolchin. A problem of the allocation of particles in cells and cycles of random permutations. *Theory of Probability & Its Applications*, 16(1):74–90, 1971.

[16] J. Pitman. Combinatorial stochastic processes. *École d'Été de Probabilités de Saint-Flour XXXII—2002*, 2006.

[17] R. M. Neal. Slice sampling. *Annals of Statistics*, 31:705–767, 2003.

[18] R. C. Steorts, S. L. Ventura, M. Sadinle, and S. E. Fienberg. A comparison of blocking methods for record linkage. In *International Conference on Privacy in Statistical Databases*, pages 253–268, 2014.

[19] M. Price, J. Klingner, A. Qtiesh, and P. Ball. Updated statistical analysis of documentation of killings in the Syrian Arab Republic, 2013. United Nations Office of the UN High Commissioner for Human Rights.

[20] M. Price, J. Klingner, A. Qtiesh, and P. Ball. Updated statistical analysis of documentation of killings in the Syrian Arab Republic. Human Rights Data Analysis Group, Geneva, 2014.

[21] S. Jain and R. Neal. A split–merge Markov chain Monte Carlo procedure for the Dirichlet process mixture model. *Journal of Computational and Graphical Statistics*, 13:158–182, 2004.

[22] L. Tierney. Markov chains for exploring posterior distributions. *The Annals of Statistics*, pages 1701–1728, 1994.

A Derivation of $P(C_N)$

In this appendix, we derive $P(C_N)$ for a general KP model, as well as the NBNB and NBD models.

A.1 KP Models

We start with equation 2 and note that

$$P(C_N) = P(C_N \mid K) P(K), \tag{13}$$

where $K = |C_N|$. To evaluate $P(C_N \mid K)$, we need to sum over all possible cluster assignments:

$$P(C_N \mid K) = \sum_{z_1,\ldots,z_N \in [K]} \underbrace{P(C_N \mid z_1,\ldots,z_N,K)}_{I(z_1,\ldots,z_N \Rightarrow C_N)} P(z_1,\ldots,z_N \mid K). \tag{14}$$

Since $N_1,\ldots,N_K$ are completely determined by K and $z_1,\ldots,z_N$, it follows that

$$P(z_1,\ldots,z_N \mid K) = P(z_1,\ldots,z_N \mid N_1,\ldots,N_K,K) P(N_1,\ldots,N_K \mid K) \tag{15}$$

$$= \frac{\prod_{k=1}^{K} N_k!}{N!} \prod_{k=1}^{K} P(N_k \mid K) \tag{16}$$

$$= \frac{1}{N!} \prod_{k=1}^{K} N_k! \, \mu_{N_k}. \tag{17}$$

Therefore,

$$P(C_N \mid K) = \sum_{z_1,\ldots,z_N \in [K]} I(z_1,\ldots,z_N \Rightarrow C_N) \frac{1}{N!} \prod_{k=1}^{K} N_k! \, \mu_{N_k} \tag{18}$$

$$= \frac{1}{N!} \left(\prod_{c \in C_N} |c|! \, \mu_{|c|} \right) \sum_{z_1,\ldots,z_N \in [K]} I(z_1,\ldots,z_N \Rightarrow C_N) \tag{19}$$

$$= \frac{K!}{N!} \prod_{c \in C_N} |c|! \, \mu_{|c|}. \tag{20}$$

Substituting equation 20 into equation 13 and using $K \sim \kappa$ we obtain

$$P(C_N) = \frac{|C_N|! \, \kappa_{|C_N|}}{N!} \left(\prod_{c \in C_N} |c|! \, \mu_{|c|} \right). \tag{21}$$

A.2 The NBNB Model

For fixed values of r and p, the NBNB model is a specific case of a KP model with

$$\kappa_k = \frac{\Gamma(k+a) \, q^k (1-q)^a}{(1-(1-q)^a) \, \Gamma(a) \, k!} \quad \text{and} \quad \mu_m = \frac{\Gamma(m+r) \, p^m (1-p)^r}{(1-(1-p)^r) \, \Gamma(r) \, m!}, \tag{22}$$

for k and m in $\mathcal{N} = \{1,2,\ldots\}$. Combining equations 21 and 22 gives

$$P(C_N \mid a,q,r,p) = \frac{|C_N|!}{N!} \frac{\Gamma(|C_N|+a) \, q^{|C_N|} (1-q)^a}{(1-(1-q)^a) \, \Gamma(a) \, |C_N|!} \prod_{c \in C_N} |c|! \frac{\Gamma(|c|+r) \, p^{|c|} (1-p)^r}{(1-(1-p)^r) \, \Gamma(r) \, |c|!} \tag{23}$$

$$= \frac{\Gamma(|C_N|+a) \, q^{|C_N|} (1-q)^a}{N! \, (1-(1-q)^a) \, \Gamma(a)} \prod_{c \in C_N} \frac{\Gamma(|c|+r) \, p^{|c|} (1-p)^r}{(1-(1-p)^r) \, \Gamma(r)}. \tag{24}$$

Conditioning on N and removing constant terms, we obtain

$$P(C_N \mid N,a,q,r,p) \propto \Gamma(|C_N|+a) \, \beta^{|C_N|} \prod_{c \in C_N} \frac{\Gamma(|c|+r)}{\Gamma(r)}, \tag{25}$$

where $\beta = \frac{q(1-p)^r}{1-(1-p)^r}$. Equation 25 leads to the following reseating algorithm:

- for $n = 1, \ldots, N$, reassign element n to
  - an existing cluster $c \in C_N \setminus n$ with probability $\propto |c| + r$
  - or a new cluster with probability $\propto (|C_N \setminus n| + a) \beta$.

Adding the prior terms for r and p to equation 24 we obtain the joint distribution of C_N, r and p:

$$
\begin{aligned}
P(C_N, r, p \,|\, a, q, \eta_r, s_r, u_p, v_p) & \\
= P(r \,|\, \eta_r, s_r) \, P(p \,|\, u_p, v_p) \, P(C_N \,|\, r, p) & \quad (26)
\end{aligned}
$$

$$
\begin{aligned}
= \frac{r^{\eta_r - 1} e^{-\frac{r}{s_r}}}{\Gamma(\eta_r) s_r^{\eta_r}} \, \frac{p^{u_p - 1}(1-p)^{v_p - 1}}{B(u_p, v_p)} \times & \\
\frac{\Gamma(|C_N| + a) \, q^{|C_N|} (1-q)^a}{N! \, (1 - (1-q)^a) \, \Gamma(a)} \prod_{c \in C_N} \frac{\Gamma(|c| + r) \, p^{|c|} (1-p)^r}{(1 - (1-p)^r) \, \Gamma(r)} & \quad (27)
\end{aligned}
$$

$$
\begin{aligned}
\propto r^{\eta_r - 1} \, e^{-\frac{r}{s_r}} \, p^{N + u_p - 1} (1-p)^{v_p - 1} \left(\frac{q(1-p)^r}{1 - (1-p)^r} \right)^{|C_N|} \times & \\
\frac{\Gamma(|C_N| + a)}{N!} \prod_{c \in C_N} \frac{\Gamma(|c| + r)}{\Gamma(r)}. & \quad (28)
\end{aligned}
$$

Therefore, the conditional posterior distributions over r and p are

$$
P(r \,|\, C_N, p, \eta_r, s_r) \propto \frac{r^{\eta_r - 1} \, e^{-\frac{r}{s_r}} \, (1-p)^{r |C_N|}}{(1 - (1-p)^r)^{|C_N|}} \prod_{c \in C_N} \frac{\Gamma(|c| - 1 + r)}{\Gamma(r)} \quad (29)
$$

$$
P(p \,|\, C_N, r, u_p, v_p) \propto \frac{p^{N + u_p - 1}(1-p)^{r |C_N| + v_p - 1}}{(1 - (1-p)^r)^{|C_N|}}. \quad (30)
$$

A.3 The NBD Model

For fixed $\boldsymbol{\mu}$, the NBD model is a specific case of a KP model. Therefore,

$$
P(C_N \,|\, a, q, \boldsymbol{\mu}) = \frac{\Gamma(|C_N| + a) \, q^{|C_N|} (1-q)^a}{N! \, (1 - (1-q)^a) \Gamma(a)} \prod_{c \in C_N} |c|! \, \mu_{|c|}. \quad (31)
$$

Conditioning on N and removing constant terms, we obtain

$$
P(C_N \,|\, N, a, q, \boldsymbol{\mu}) \propto \Gamma(|C_N| + a) \, q^{|C_N|} \prod_{c \in |C_N|} |c|! \, \mu_{|c|}.
$$

Via Dirichlet–multinomial conjugacy,

$$
\boldsymbol{\mu} \,|\, C_N, \alpha, \boldsymbol{\mu}^{(0)} \sim \mathrm{Dir}\left(\alpha \, \mu_1^{(0)} + L_1, \alpha \, \mu_2^{(0)} + L_2, \ldots \right), \quad (32)
$$

where L_m is the number of clusters of size m in C_N. Although $\boldsymbol{\mu}$ is an infinite-dimensional vector, only the first N elements affect $P(C_N \,|\, a, q, \boldsymbol{\mu})$. Therefore, it is sufficient to sample the $(N+1)$-dimensional vector $(\mu_1, \ldots, \mu_N, 1 - \sum_{m=1}^N \mu_m)$ from equation 32, modified accordingly:

$$
(\mu_1, \ldots, \mu_N, 1 - \sum_{m=1}^N \mu_m) \,|\, C_N, \alpha, \mu_1^{(0)}, \ldots, \mu_N^{(0)}
$$

$$
\sim \mathrm{Dir}\left(\alpha \, \mu_1^{(0)} + L_1, \ldots, \alpha \, \mu_N^{(0)} + L_N, \alpha \left(1 - \sum_{m=1}^N \mu_m^{(0)} \right) \right). \quad (33)
$$

We can then discard $1 - \sum_{m=1}^N \mu_m$.

B   Proof of the Microclustering Property for a Variant of the NBNB Model

Theorem 1. *If C_N is drawn from a KP model with $\boldsymbol{\kappa} = NegBin\,(a, q)$ and $\boldsymbol{\mu} = NegBin\,(r, p)$,*[6] *then for all $\epsilon > 0$, $P(M_N \,/\, N \geq \epsilon) \to 0$ as $N \to \infty$, where M_N is the size of the largest cluster in C_N.*

In this appendix, we provide a proof of theorem 1.

We use the following fact: $\Gamma\,(x + a) \,/\, \Gamma\,(x) \asymp x^a$ as $x \to \infty$ for any $a \in \mathbb{R}$ via Stirling's approximation to the gamma function. We use $f(x) \asymp g(x)$ to denote that $f(x) \,/\, g(x) \to 1$ as $x \to \infty$.

Lemma 1. *For any $k \in \{1, 2, \ldots\}$, $P(K = k \,|\, N = n) \to 0$ as $n \to \infty$.*

Proof. Because $N \,|\, K = k \sim \mathrm{NegBin}\,(kr, p)$,

$$P(K = k, N = n) = \frac{\Gamma\,(k + a)}{k!\,\Gamma\,(a)}\,(1 - q)^a\,q^k\,\frac{\Gamma\,(n + kr)}{n!\,\Gamma\,(kr)}\,(1 - p)^{kr}\,p^n.$$

Via the fact noted above, $\Gamma\,(n + kr) \,/\, \Gamma\,(n + kr + r) \asymp 1 \,/\, (n + kr)^r \to 0$ as $n \to \infty$, so

$$\frac{P(K = k, N = n)}{P(K = k + 1, N = n)} = \frac{\Gamma\,(k + a)\,(k + 1)}{\Gamma\,(k + a + 1)\,q}\,\frac{\Gamma\,(kr + r)}{\Gamma\,(kr)}\,\frac{\Gamma\,(n + kr)}{\Gamma\,(n + kr + r)} \to 0 \text{ as } n \to \infty.$$

Therefore,

$$P(K = k \,|\, N = n) = \frac{P(K = k, N = n)}{\sum_{k'=0}^{\infty} P(K = k', N = n)} \leq \frac{P(K = k, N = n)}{P(K = k + 1, N = n)} \to 0.$$

$\square$

Lemma 2. *For any $\epsilon \in (0, 1)$, there exist $c_1, c_2, \ldots \geq 0$, not depending on n, such that $c_k \to 0$ as $k \to \infty$ and $k\,P(N_1 \,/\, n \geq \epsilon \,|\, K = k, N = n) \leq c_k$ for all $n \geq 2 \,/\, \epsilon$ and $k \in \{1, 2, \ldots\}$.*

Before proving lemma 2, we first show how theorem 1 follows from it.

Proof of theorem 1. Let $\epsilon \in (0, 1)$ and choose $c_1, c_2, \ldots$ by lemma 2. For any $n \geq 2 \,/\, \epsilon$,

$$P(M_n \,/\, n \geq \epsilon \,|\, N = n)$$

$$= \sum_{k=1}^{\infty} P(N_1 \,/\, n \geq \epsilon \text{ or } \cdots \text{ or } N_K \,/\, n \geq \epsilon \,|\, K = k, N = n)\,P(K = k \,|\, N = n)$$

$$\leq \sum_{k=1}^{\infty} \sum_{i=1}^{k} P(N_i \,/\, n \geq \epsilon \,|\, K = k, N = n)\,P(K = k \,|\, N = n)$$

$$= \sum_{k=1}^{\infty} k\,P(N_1 \,/\, n \geq \epsilon \,|\, K = k, N = n)\,P(K = k \,|\, N = n)$$

$$\leq \sum_{k=1}^{\infty} c_k\,P(K = k \,|\, N = n) \leq \sup\{c_k : k > m\} + \sum_{k=1}^{m} c_k\,P(K = k \,|\, N = n)$$

for any $m \geq 1$. (We note that we only summed over $k \geq 1$ because $P(K = 0 \,|\, N = n) = 0$ for any $n \geq 1$.) Therefore, via lemma 1, $\limsup_n P(M_n \,/\, n \geq \epsilon \,|\, N = n) \leq \sup\{c_k : k > m\}$. Finally, because $\sup\{c_k : k > m\} \to 0$ as $m \to \infty$, theorem 1 follows directly from lemma 2, as desired. $\square$

To prove lemma 2, we need two supporting results.

Lemma 3. *If $b > (r + 1) \,/\, r$ and $\theta_k \sim Beta\,(r, (k - 1)\,r)$, then $k\,P(\theta_k \geq \frac{b\log\,(k)}{k}) \to 0$ as $k \to \infty$.*

Proof. Let $a_k = (b\log\,(k)) \,/\, k$, and suppose that k is large enough that $a_k \in (0, 1)$. First, for any $\theta \in (a_k, 1)$, we have $\theta^{r-1} \leq 1 \,/\, a_k$. Second, $B\,(r, (k - 1)\,r) = \Gamma\,(r)\,\Gamma\,(kr - r) \,/\, \Gamma\,(kr) \asymp$

---

[6]We have not truncated the negative binomial distributions, so this is a minor variant the NBNB model.

$\Gamma\left(r\right)\left(kr\right)^{-r}$ as $k \to \infty$, via Stirling's approximation, as we noted previously. Third, because $1 + x \le \exp\left(x\right)$ for any $x \in \mathbb{R}$, $\left(1 - a_k\right)^{kr} \le \exp\left(-a_k\right)^{kr} = k^{-rb}$. Therefore, we obtain

$$k\, P(\theta_k \ge a_k)$$

$$= \frac{k}{B\left(r, (k-1)\, r\right)} \int_{a_k}^1 \theta^{r-1} \left(1 - \theta\right)^{(k-1)\, r - 1} \mathrm{d}\theta$$

$$\le \frac{k\,/\, a_k}{B\left(r, (k-1)\, r\right)} \int_{a_k}^1 \left(1 - \theta\right)^{(k-1)r - 1} \mathrm{d}\theta = \frac{k\,/\, a_k}{B\left(r, (k-1)\, r\right)} \frac{\left(1 - a_k\right)^{(k-1)\, r}}{(k-1)\, r}$$

$$\le \frac{k\,/\, a_k}{B\left(r, (k-1)\, r\right)} \frac{k^{-rb} \left(1 - a_k\right)^{-r}}{(k-1)\, r} \asymp \frac{k^2\,/\, (b\log\left(k\right))}{\Gamma\left(r\right)\left(kr\right)^{-r}} \frac{k^{-rb}}{kr} = \frac{r^{r-1}\, k^{-br+r+1}}{\Gamma\left(r\right)\left(b\log\left(k\right)\right)} \to 0$$

as $k \to 0$ because $b > (r+1)\,/\, r$. $\qquad\square$

Lemma 4. *Let $b > 0$ and $\epsilon \in (0,1)$, as well as $k > 1$ and $n \in \{1, 2, \ldots\}$. If $(b\log\left(k\right))\,/\, k < 1$ and $X \sim \mathrm{Bin}\left(n, (b\log\left(k\right))\,/\, k\right)$, then $P(X \ge n\epsilon) \le \left(1 + b\log\left(k\right)\right)^n\,/\, k^{n\epsilon}$.*

Proof. Let $Z_1, \ldots, Z_n \overset{\text{iid}}{\sim} \mathrm{Bern}\left((b\log\left(k\right))\,/\, k\right)$. Because $x \mapsto k^x$ is strictly increasing,

$$P(X \ge n\epsilon) = P(k^X \ge k^{n\epsilon}) \le \frac{\mathbb{E}[k^X]}{k^{n\epsilon}} = \frac{\prod_{i=1}^n \mathbb{E}[k^{Z_i}]}{k^{n\epsilon}} \le \frac{\left(1 + b\log\left(k\right)\right)^n}{k^{n\epsilon}}$$

via Markov's inequality. $\qquad\square$

Proof of lemma 2. First, let $\epsilon \in (0,1)$. Next, let $b = (r+2)\,/\, r$ and choose $k^* \in \{2, 3, \ldots\}$ to be sufficiently large that $(1 + b\log\left(k\right))\,/\, k^\epsilon < 1$ and $(b\log\left(k\right))\,/\, k < \epsilon$ for all $k \ge k^*$. Then, for $k = 1, 2, \ldots, k^* - 1$, define $c_k = k$, and, finally, for $k = k^*, k^* + 1, \ldots$, define

$$c_k = k^{-1}(1 + b\log\left(k\right))^{2/\epsilon} + k\, P\left(\theta_k \ge \frac{b\log\left(k\right)}{k}\right),$$

where $\theta_k \sim \mathrm{Beta}\left(r, (k-1)\, r\right)$.

Via lemma 3, $c_k \to 0$ as $k \to \infty$. Trivially, for $k < k^*$, $k\, P(N_1\,/\, n \ge \epsilon \mid K = k, N = n) \le k = c_k$.

Let $k \ge k^*$ and suppose that $n \ge 2\,/\,\epsilon$. Via a straightforward calculation, we can show that $N_1 \mid K = k, N = n \sim \mathrm{BetaBin}\left(n, r, (k-1)\, r\right)$. (This follows from the fact that if $Y \sim \mathrm{NegBin}\left(r, p\right)$ and, independently, $Z \sim \mathrm{NegBin}\left(r', p\right)$, then $Y \mid (Y + Z) = n \sim \mathrm{BetaBin}\left(n, r, r'\right)$.) Therefore, if we define $\theta \sim \mathrm{Beta}\left(r, (k-1)\, r\right)$, $X \mid \theta \sim \mathrm{Bin}\left(n, \theta\right)$, and $a = (b\log\left(k\right))\,/\, k$, then we have

$$k\, P(N_1\,/\, n \ge \epsilon \mid K = k, N = n) = k\, P(X \ge n\epsilon)$$
$$= k\, P(X \ge n\epsilon, \theta < a) + k\, P(X \ge n\epsilon, \theta \ge a).$$

However, $k\, P(X \ge n\epsilon, \theta \ge a) \le k\, P(\theta \ge a) = k\, P\left(\theta_k \ge \frac{b\log\left(k\right)}{k}\right)$. To handle the first term, we note that as a function of θ, $P(X = x \mid \theta)$ is nondecreasing on $(0, \epsilon)$ whenever $x\,/\, n \ge \epsilon$ because $\frac{\mathrm{d}P(X = x \mid \theta)}{\mathrm{d}\theta} = \binom{n}{x} \theta^{x-1} \left(1 - \theta\right)^{n-x-1} (x - n\theta)$. Therefore, $P(X \ge n\epsilon \mid \theta) = \sum_{x \ge n\epsilon} P(X = x \mid \theta)$ is nondecreasing on $(0, \epsilon)$. Finally, because our choice of k^* means that $a \in (0, \epsilon)$,

$$k\, P(X \ge n\epsilon, \theta < a)$$

$$= k \int_0^a P(X \ge n\epsilon \mid \theta)\, P(\theta)\, \mathrm{d}\theta \le k\, P(X \ge n\epsilon \mid \theta = a)$$

$$\le k\, \left(1 + b\log\left(k\right)\right)^n\,/\, k^{n\epsilon} = k\, \left(\frac{1 + b\log\left(k\right)}{k^\epsilon}\right)^n$$

$$\le k\, \left(\frac{1 + b\log\left(k\right)}{k^\epsilon}\right)^{2/\epsilon} = k^{-1}\, \left(1 + b\log\left(k\right)\right)^{2/\epsilon},$$

where the second inequality is via lemma 4 and the third inequality holds because $n \ge 2\,/\,\epsilon$ and $(1 + b\log\left(k\right))\,/\, k^\epsilon < 1$ because of our choice of k^*. Thus, $k\, P(N_1\,/\, n \ge \epsilon \mid K = k, N = n) \le c_k$. $\quad\square$

This completes the proof of theorem 1.

C The Chaperones Algorithm

For large data sets with many small clusters, standard Gibbs sampling algorithms (such as the one outlined in section 3) are too slow. In this appendix, we therefore propose a new Gibbs-type sampling algorithm, which we call the chaperones algorithm. This algorithm is inspired by existing split–merge Markov chain sampling algorithms [21, 4, 6]; however, it is simpler, more efficient, and—most importantly—likely exhibits better mixing properties when there are many small clusters.

In a standard Gibbs sampling algorithm, each iteration involves reassigning each data point x_n for $n = 1, \ldots, N$ to an existing cluster or to a new cluster by drawing a sample from $P(C_N \mid N, C_N \setminus n, x_1, \ldots, x_N)$. When the number of clusters is large, this step can be inefficient because the probability that element n will be reassigned to a given cluster will, for most clusters, be extremely small.

The chaperones algorithm focuses on reassignments that have higher probabilities. If $c_n \in C_N$ denotes the cluster containing data point x_n, then each iteration consists of the following steps:

1. Randomly choose two chaperones, $i, j \in \{1, \ldots, N\}$ from a distribution $P(i, j \mid x_1, \ldots, x_N)$ where the probability of i and j given $x_1, \ldots, x_N$ is greater than zero for all $i \neq j$. This distribution must be independent of the current state of the Markov chain C_N; however, crucially, it may depend on the observed data points $x_1, \ldots, x_N$.

2. Reassign each $x_n \in c_i \cup c_j$ by sampling from $P(C_N \mid N, C_N \setminus n, c_i \cup c_j, x_1, \ldots, x_N)$.

In step 2, we condition on the current partition of all data points except x_n, as in a standard Gibbs sampling algorithm, but we also force the set of data points in $c_i \cup c_j$ to remain unchanged—i.e., x_n must remain in the same cluster as at least one of the chaperones. (If n is a chaperone, then this requirement is always satisfied.) In other words, we view the non-chaperone data points in $c_i \cup c_j$ as "children" who must remain with a chaperone at all times. Step 2 is almost identical to the restricted Gibbs moves found in existing split–merge algorithms, except that the chaperones i and j can also change clusters, provided they do not abandon any of their children. Splits and merges can therefore occur during step 2: splits occur when one chaperone leaves to form its own cluster; merges occur when one chaperone, belonging to a singleton cluster, then joins the other chaperone's cluster.

The chaperones algorithm can be justified as follows: For any fixed pair of chaperones (i, j), step 2 is a sequence of Gibbs-type moves and therefore has the correct stationary distribution. Randomly choosing the chaperones in step 1 amounts to a random move, so, taken together, steps 1 and 2 also have the correct stationary distribution (see, e.g., [22], sections 2.2 and 2.4). To guarantee irreducibility, we start by assuming that $P(x_1, \ldots, x_N \mid C_N) \, P(C_N) > 0$ for any C_N and by letting C'_N denote the partition of N in which every element belongs to a singleton cluster. Then, starting from any partition C_N, it is easy to check that there is a positive probability of reaching C'_N (and vice versa) in finitely many iterations; this depends on the assumption that $P(i, j \mid x_1, \ldots, x_N) > 0$ for all $i \neq j$. Aperiodicity is also easily verified since the probability of staying in the same state is positive.

The main advantage of the chaperones algorithm is that it can exhibit better mixing properties than existing sampling algorithms. If the distribution $P(i, j \mid x_1, \ldots, x_N)$ is designed so that x_i and x_j tend to be similar, then the algorithm will tend to consider reassignments that have a relatively high probability. In addition, the algorithm is easier to implement and more efficient than existing split–merge algorithms because it uses Gibbs-type moves, rather than Metropolis-within-Gibbs moves.

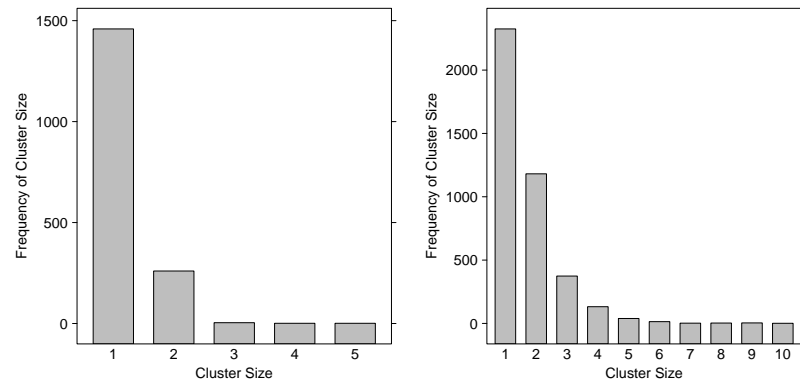# D The Syria2000 and SyriaSizes Data Sets

Figure 3: Cluster size distributions for the Syria2000 (left) and SyriaSizes (right) data sets.